Clin Pharmacol Ther. Author manuscript; available in PMC 2016 April 25.

Published in final edited form as:
Clin Pharmacol Ther. 2013 October ; 94(4): 533–543. doi:10.1038/clpt.2013.122.

Profiling serum bile acid glucuronides in humans: gender divergences, genetic determinants and response to fenofibrate

Jocelyn Trottier[1], **Martin Perreault**[1], **Iwona Rudkowska**[2], **Cynthia Levy**[3], **Amélie Dallaire-Theroux**[1], **Mélanie Verreault**[1], **Patrick Caron**[1], **Bart Staels**[4], **Marie-Claude Vohl**[2], **Robert J. Straka**[5], and **Olivier Barbier**[1]

[1]Laboratory of molecular pharmacology, Endocrinology and Nephrology, CHU-Québec Research Centre and the Faculty of pharmacy, Laval University, Québec, Canada

[2]Nutraceuticals and Functional Foods Institute (INAF) and Endocrinology and Nephrology, CHU-Québec Research Centre, Québec, Canada

[3]Division of Gastroenterology, Hepatology and Nutrition, Department of Medicine, University of Florida, Gainesville, FL, USA

[4]INSERM-U1011; Institut Pasteur de Lille and Université Lille, Lille, France

[5]Experimental and Clinical Pharmacology Department, College of Pharmacy, University of Minnesota, Minneapolis, MN, USA

Abstract

Glucuronidation, catalyzed by UDP-glucuronosyltransferase (UGT) enzymes detoxifies cholestatic bile acids (BAs). We aimed at *i)* characterizing the circulating BA-glucuronide (-G) pool composition in humans, *ii)* evaluating how sex and UGT polymorphisms influence this composition, and *iii)* analyzing the effects of lipid-lowering drug fenofibrate on the circulating BA-G profile in 300 volunteers and 5 cholestatic patients. Eleven BA-Gs were determined in pre- and post-fenofibrate samples. Men exhibited higher BA-G concentrations, and various genotype/BA-G associations were discovered in relevant UGT genes. The chenodeoxycholic acid-3G concentration was associated with the UGT2B7 802C>T polymorphism. Glucuronidation assays confirmed the predominant role of UGT2B7 and UGT1A4 in CDCA-3G formation. Fenofibrate exposure increased the serum levels of 5 BA-G species, including CDCA-3G, and up-regulated expression of UGT1A4, but not UGT2B7, in hepatic cells. This study demonstrates that

Contact informations: Olivier Barbier, Ph. D., Laboratory of molecular pharmacology, CHU-Québec Research Centre, 2705 Laurier Boulevard, Québec (QUE) G1V 4G2 CANADA. Phone: 418 654 2296. Fax: 418 654 2761. olivier.barbier@crchul.ulaval.ca.

CONFLICT OF INTERESTS/DISCLOSURE
Authors have nothing to disclose.

SPECIFIC AUTHOR CONTRIBUTIONS
All authors are justifiably credited with authorship, according to authorship criteria.
OB, CL, BS, MCV, RJS designed the research
JT, MP, ADT, MV, PC performed the research
JT, MP, ADT, MV, PC, IR, OB, CL, BS, MCV, RJS analyzed the data
JT, OB wrote the mansucript

fenofibrate stimulates BA glucuronidation in humans, and thus reduces bile acid toxicity in the liver.

Keywords

Cholestasis; fibrates; bile acid detoxification; mass spectrometry; UDP-glucuronosyltransferase

INTRODUCTION

Bile acids (BAs) are natural detergents involved in cholesterol homeostasis (1). These acids are formed from cholesterol in the liver and their synthesis represents an important pathway for cholesterol elimination from the body (1). In humans, the bile acid pool is mainly composed by the primary cholic (CA) and chenodeoxycholic acids (CDCA), the secondary lithocholic (LCA) and deoxycholic (DCA) acids, and the 6α-hydroxylated hyocholic (HCA) and hyodeoxycholic acids (HDCA) (1, 2). BAs sustain a strong enterohepatic recirculation, through which they are excreted from the liver into the bile, stored in gallbladder and secreted in the intestine where they serve as natural detergents for dietary lipids absorption (1). Approximately 95% of bile acids are absorbed in the intestine and return to the liver through the portal vein. BAs are cytotoxic at high concentrations (3), and their accumulation in liver cells leads to oxidative stress, apoptosis and subsequent damage to the liver parenchyma (1). Such features are characteristic of cholestatic phenomena, where a reduction of the bile flow limits BA elimination from hepatocytes (4). A reduction of BA hepatic levels is therefore an important goal for anti-cholestatic strategies (5), particularly for the treatment of chronic situations such as primary biliary cirrhosis (PBC) or primary sclerosing cholangitis (PSC), two autoimmune hepatobiliary diseases (1).

Glucuronidation, catalyzed by UDP-glucuronosyltransferase (UGT) enzymes, is a major detoxification pathway for numerous endo- and xenobiotics. This conjugation reaction transfers a highly hydrophilic glucuronide group to hydrophobic molecules. The resulting glucuronide products are therefore more easily excreted and consequently less toxic than the substrate molecules (reviewed in (6)). Glucuronidation allows the carrying of BAs into the blood by conjugate transporters at the basolateral membrane of hepatocytes for subsequent elimination into the urine (6). Based on this re-routing, BA-conjugating enzymes have been proposed as novel targets for future anti-cholestatic drugs (6, 7). Amongst the 19 human functional UGTs, UGT1A3, UGT2B4 and UGT2B7 have a remarkable capacity to convert BAs into BA-glucuronides (BA-G) *in vitro* (reviewed in (6)); however, our understanding of their contribution to BA detoxification in clinics is currently limited. Indeed, BA-Gs are rarely investigated in humans, and very little is known about the circulating BA-G pool composition.

Amongst the newly identified therapeutic approaches for chronic cholestasis, the cholesterol-lowering fibrates (fenofibrate, bezafibrate and clofibrate) improve liver biochemistries in PBC and PSC patients (8–13). These beneficial effects were associated to classical fibrate actions on lipoprotein metabolism and anti-inflammatory processes (reviewed in (14)). However, as pharmacological activators for the peroxisome proliferator–

activated receptor-α (PPARα), these drugs also control BA metabolism (reviewed in (15)). PPARα is a ligand-activated transcription factor controlling the expression of target genes through binding to their regulatory regions as a heterodimer with the Retinoid X-receptor (RXR) (15). For example, upon fibrate activation, PPARα binds to and stimulates expression of the genes encoding the 2 BA-conjugating UGT1A3 and UGT2B4 enzymes in human liver cells and animal models (16–18). On the other hand, we recently observed that fenofibrate reduces circulating BA concentrations in non–cholestatic volunteers (2). The present study aimed at investigating the possibility that such a reduction actually reflects an increased BA glucuronidation. For this purpose, the profile of circulating BA-G was established and compared in pre- and post-fenofibrate sera from 150 men and 150 women volunteers. Similar analyses were also conducted in a pilot study comprising 5 fenofibrate-treated PBC patients. How the non-cholestatic BA-G profile and it response to fenofibrate is affected by the gender or non-synonymous mutations BA-conjugating UGT genes was also examined. These analyses evidenced the need for additional *in vitro* and *ex vivo* experiments aimed at establishing the relative contribution of human UGTs for the hepatic formation of abundant BA-G species, and at measuring the reactivity of their functional variants. Finally, whether PPARα also controls the expression of these newly identified BA-conjugating UGTs has been investigated in hepatic cells.

RESULTS

Serum profile of bile acid glucuronides, gender-related differences and association with common UGT2B4, UGT2B7 and UGT1A3 gene polymorphisms in non-cholestatic volunteers

Composition of the serum bile acid glucuronide pool is illustrated in Table 1. The species distribution was: HCA-6G≥CDCA-3G>HDCA-6G>DCA-3G≫CA-24G=LCA-3G>LCA-24G≥HCA-24G≥DCA-24G=CDCA-24G=HDCA-24G. The hydroxyl-linked glucuronidated acids (i.e. -3G and -6G) represented 96.5% of the circulating BA-G pool; and the 4 most abundant conjugates (HCA-6G, CDCA-3G, HDCA-6G and DCA-3G) represented more than 95% of the BA-G detected in the human serum.

A comparison of the baseline BA-G profiles in men and women revealed that female sera contained a significantly lower amount of CDCA-3G ($p<0.001$), LCA-3G ($p<0.05$), HDCA-6G ($p<0.05$) and HCA-6G ($p<0.001$). As a consequence, the total BA-G ($p<0.001$) was also significantly lower in women sera (Table 1).

Genotyping for previously identified non-synonymous mutations within the BA-conjugating UGTs (19–24) (SI5–7) revealed that the UGT1A3 31T>C genotype significantly influences LCA-24G (Fig. 1A, T/T being different from T/C and C/C values, $p<0.005$), as well as the level of carboxyl-linked glucuronidated acids (i.e. -24G) (Fig. 1B, T/T different from T/C values, $p<0.05$). The UGT2B7 802C>T genotype associates with significant differences changes in CDCA-3G concentration (Fig. 1C, C/C lower than CT values, $p<0.05$), while HDCA-24G levels were significantly reduced in UGT2B4 1374T/T carriers (Fig. 1D, T/T lower than A/T and T/T values, $p<0.05$). To ensure that changes in BA-G serum levels reflected variations in glucuronide formation, we calculated the relative abundance

(percentage of BAG/BA+BA-G) of glucuronide conjugates and the metabolic ratio (ratio glucuronide *versus* its unconjugated precursor) for each species. While MRs varied from 0.01 (DCA-24G/DCA) to 8.9 (HCA-6G/HCA) (Table 1), the sum of BA-G species account for 8.5% of the total bile acid pool in human serum (Fig. 3E). Only the ratio HDCA-6G/HDCA was found significantly higher ($p<0.05$) in men than in women (Table 1), and the unique significant gene association concerned the UGT2B7 $Y^{268}H$ variant: carriers of the 802 C/T genotype presented a significantly higher HCA-6G/HCA ratio (12.12) than those with the C/C (9.76) ($p<0.05$) (SI5).

These observations indicate that *i)* glucuronide conjugates represent almost 10% of the circulating BA pool in humans; *ii)* HCA-6G, CDCA-3G, HDCA-6G and DCA-3G are the most abundant species; and *iii)* serum levels of selected BA-G species are significantly linked to non-synonymous mutations in genes encoding BA-conjugating UGTs.

UGT1A4 and UGT2B7 catalyze hepatic formation of CDCA-3G

Until now, CDCA-3G was considered a minor CDCA metabolite, due to its limited production observed *in vitro* with human liver extracts. Consequently, the mechanisms governing its formation received only little attention (17). In this context, an *in vitro* screening was performed with human liver microsomes and recombinant UGTs (Fig. 2). As previously reported (17), the formation of CDCA-3G was detected in the presence of liver microsomes, but at a 8.3-fold lower level than the production of CDCA-24G in the same assay (Fig. 2A). Assays with UGT-bacculosomes revealed the predominant contribution of the UGT1A4 and UGT2B7 isoforms in producing CDCA-3G (Fig. 2B). To determine whether frequent (≥1%) non-synonymous mutations in the coding region of these enzymes affect their ability to convert CDCA into CDCA-3G (25, 26), additional assays were performed with microsomes from HK293 cells stably expressing the WT ($R^{11}P^{24}L^{48}$) or variant UGT1A4 T^{24}, V^{48} and W^{11} proteins, as well as the WT H^{268} or Y^{268} UGT2B7 enzymes (Fig. 2C–F) (25, 26). Activity values were adjusted for UGT1A4 or UGT2B7 protein content as determined by western-blot (Fig. 2C&D) (26). All UGT1A4 variants exhibited a similar CDCA-3G formation (Fig. 2E), while the UGT2B7 Y^{268} protein was 1.3-fold more active than the H^{268} allozyme ($p<0.05$) (Fig. 2F).

These *in vitro* analyses identify UGT1A4 and UGT2B7 as major enzymes for hepatic CDCA-3G formation.

Fenofibrate causes an accumulation of selected bile acid-glucuronide species in sera from non cholestatic and PBC donors

Treatment with fenofibrate resulted in a significant increase ($p<0.001$) of the total glucuronide concentration in GOLDN donors (Fig. 3A). Such induction reflected the 88% increase in HDCA-6G levels ($p<0.001$), but also the accumulation of HDCA-24G ($p<0.001$), HCA-6G ($p<0.001$), HCA-24G ($p<0.001$) and CA-24G ($p<0.001$) (Fig. 3B–D). LCA-3G (−10%) was the unique species negatively affected by fenofibrate (Fig. 3D, $p<0.01$). Other species (i.e CDCA-3 and 24G, DCA-3 and 24G, and LCA-24G) were not significantly altered, even if CDCA-3G tended to increase (+13%, $p=0.07$, Fig. 3B). The unique difference in the response to fenofibrate between men and women corresponded to the

LCA-3G reduction which reached statistical significance only in men (SI8). Significant interactions were observed for the UGT2B7H^{268}Y genotype: CDCA-3G and CA-24G levels were significantly increased by fenofibrate in samples from C/C donors, while carriers of the C/T genotype remained not responsive (SI8).

In these donors, fenofibrate also significantly increased the relative abundance of BA-G within the serum BA pool (Fig. 3E, $p<0.001$), as well as the metabolic ratios for CDCA-3G ($p<0.001$), DCA-3G ($p<0.001$) and -24G ($p<0.05$), LCA-24G ($p<0.05$), HDCA-6G ($p<0.001$) and -24G ($p<0.001$), HCA-6G ($p<0.01$) (Fig. 3F–I). The most impressive changes were observed for HDCA-6G and -24G (Fig. 3F&I). Interestingly, the fenofibrate-dependent changes in LCA-3G and HCA-24G species (Fig. 3C&D) did not result in significant modulation of their MRs (Fig. 3H). In the same vein, not only did the increased concentration of circulating CA-24G not lead to an increase in its MR, but this ratio was even significantly reduced (Fig. 3H, $p<0.01$). Finally, metabolic ratios for DCA-24G and HCA-6G were differentially affected in men and women (SI8).

To investigate whether fenofibrate also affects the circulating BA-G profile in cholestatic patients, a pilot study was performed with samples from 5 fenofibrate-supplemented PBC patients (SI9&Fig. 4). The great inter-individual variability and the small population size drastically reduced the statistical significance of the following observations. Nevertheless, it is remarkable that fenofibrate exerted similar effects as in non cholestatic donors, since 4 out of 5 donors presented increase in the total BA-G concentration (Fig. 4A). Circulating CDCA-3G (Fig. 4B), HDCA-6G (Fig. 4C) and HCA-6G (Fig. 4D) levels were increased after fenofibrate exposure but only in 3, 3 and 2 donors, respectively.

These results demonstrate that fenofibrate increases serum BA-G in healthy donors and PBC patients.

PPARα activation up-regulates UGT1A4, but not UGT2B7, expression in human hepatic cells

We next investigated whether hepatic expression of known (UGT2B4, UGT2B7 and UGT1A3) or newly identified (UGT1A4) BA-conjugating enzymes were affected by the PPARα agonist, fenofibrate and Wy14,643 (Fig. 5). According to previous reports (16, 17), both activators up-regulated UGT1A3 and UGT2B4 mRNA expression in human hepatocytes and hepatoma HepG2 cells (Fig. 5A–C). Interestingly, the 2 CDCA-3G-forming enzymes were differentially affected: UGT1A4 was induced in fenofibrate- and Wy14,643-treated hepatocytes, while UGT2B7 mRNA levels remained unaffected (Fig. 5A&B). The dose- and time-dependent, as well the transcriptional and direct nature of the Wy14,643-dependent UGT1A4 activation was confirmed in dose response (Fig. 5C), time course experiments (Fig. 5D) and by the concomitant use of inhibitors for gene transcription (actinomycin D) or mRNA traduction (cycloheximide) (Fig. 5E). Accordingly to previous reports (17, 27), glucuronidation assays performed with human hepatocytes exposed or not to Wy14,643 (75μM) resulted in a 2-fold increased CDCA-24G production (Fig. 5F). A similar increase was observed with CDCA-3G formation, however the glucuronide production of control and treated cells were below the limit of quantification of the LC-MS/MS method, which is also in accordance with previous studies reporting the

predominant conversion of CDCA into its acyl glucuronide conjugates in human liver cells (17, 27).

These observations demonstrate that PPARα activators stimulate the expression of 3 out of the 4 human BA-glucuronidating enzymes.

Bile acid glucuronides are less cytotoxic than their unconjugated precursors in HepG2 cells

Since some glucuronides, such as LCA-3G, can exert toxic and/or cholestatic effects (28), we next investigated whether the abundant CDCA-3G and the potentially toxic LCA-3G affect hepatoma HepG2 cells viability(Fig. 5G&H). When compared to their unconjugated precursors used at the same dose (100μM), LCA-3G and CDCA-3G failed to cause any alteration of cell viability in MTS reduction assays (Fig. 5G). When living cells were discriminated by FACS, the 2 glucuronides also revealed less cytotoxicity than their precursors (Fig. 5H).

DISCUSSION

The present study provides the first comprehensive analysis of the bile acid-glucuronide profile in human sera, and its response to fenofibrate.

Together 4 species, HCA-6G, HDCA-6G, CDCA-3G and DCA-3G represent 95 and 89% of all the BA-G pool in normal and PBC sera, respectively. HDCA-6G and HCA-6G are efficiently formed by the human liver (15, 29), and these species were expected to be abundant in human serum. By contrast, CDCA-3G and DCA-3G are minimally produced *in vitro* (15, 17, 30). Actually, the major products in glucuronidation assays correspond to CDCA-24G and DCA-24G (15, 17, 30), 2 C_{24} acyl-glucuronides detected at very low serum concentrations in the present study. Such a paradoxical situation was foretold by A. Hofmann (31), who proposed that the C_{24} carboxyl group of bile acid molecules is preferentially used for glycine or taurine conjugation *in vivo,* thus precluding its use for glucuronidation (17, 29, 31). It is, however, also possible that the C_{24} BA-G formed in the human liver cannot be efficiently detected in the blood due to an extensive degradation. Actually, acyl glucuronide conjugates are instable at physiological pH and their abundance is usually underestimated (32–34). Accordingly, we previously observed that incubation of C_{24} BA-G in neutral to basic solutions for 2H results in a strong reduction of the glucuronide concentrations (30). Whether acyl-BA-Gs are underestimated due to degradation or if their low levels reflect a reduced formation still remains to be clarified.

Women display lower CDCA-3G, HDCA-6G and HCA-6G levels than men, and consequently exhibit a reduced total BA-G concentration. This observation is consistent with the previous report that bile acid species, such as CDCA and HCA, are more abundant in men than in women (2). Thus, the higher CDCA-3G and HCA-6G concentrations may only reflect an improved availability of these acids for glucuronidation in the male liver. By contrast, HDCA concentrations were previously found identical in male and female sera from the GOLDN study (2), suggesting that conversion of HDCA into this glucuronide derivative is favored in men. Accordingly, the MRs for CDCA-3G and HCA-6G were not

influenced by the gender, while men also exhibited a higher HDCA-6G/HDCA ratio than women. Actually, gender-related differences in glucuronidation rates have been often reported and appear dependent on gender-specific growth and sex hormones secretions (35).

The UGT1A3 31T>C polymorphism influences baseline carboxyl-linked BA-G levels, thus confirming *in vivo* the previous *in vitro* characterization of UGT1A3 as a specialized enzyme for acyl glucuronidation of BAs (17, 29, 36–38). More surprising was the significant association between the UGT2B4 1374T>A polymorphism and HDCA-24G concentration. Indeed, this enzyme is by far more efficient in converting HDCA into HDCA-6G than into HDCA-24G (15, 23, 37, 39, 40). Interestingly, HDCA-6 and -24G levels sustain a similar accumulation in donors carrying the A1374 allele, but only the HDCA-24G variation reaches the statistical significance. It is therefore likely that the functional impact of the resulting UGT2B4 $D^{458}E$ amino acid change reaches statistical significance only for low efficiency catalytic reactions. On the other hand, CDCA-3G levels were significantly associated to the UGT2B7 802C>T polymorphism, which suggested an important role for this enzyme in converting CDCA into CDCA-3G. This was further confirmed through the *in vitro* screening experiments. Indeed, among the recombinant UGTs tested, only UGT2B7 and UGT1A4 were efficient in producing CDCA-3G. Actually, our data support complementary roles for these 2 isoforms: UGT2B7 being predominant for baseline CDCA-3G levels, while UGT1A4 may be responsible for its increased production upon fenofibrate exposure. Indeed, *in vitro* assays confirmed the functional impact of the UGT2B7 802C>T mutation on CDCA-3G formation, where none of the common UGT1A4 variants tested exhibited altered activity. By contrast, the improved UGT1A4 expression in PPARα-activated hepatic cells identifies the UGT1A enzyme as responsible for the increased CDCA-3G/CDCA ratio observed in post-fenofibrate serum samples (Fig. 6). In the same vein, while both UGT2B4 and UGT2B7 efficiently convert HDCA and HCA into 6-glucuronide conjugates *in vitro* (37), the increased HDCA-6 and HCA-6G concentrations in post-fenofibrate sera likely reflects the PPARα-dependent activation of UGT2B4 expression (Fig. 6).

Last, but not least, the present study also evidences BA glucuronidation as a deeply fenofibrate-regulated process in humans. Indeed, among the 11 BA-G species analyzed, 5 were significantly increased in post-treatment samples and 6 exhibited higher MR values. Within the total of 28 BA species analyzed until now (i.e. 17 non glucuronides (2) + 11 glucuronides), the most impressive change caused by fenofibrate corresponds to the 88% increase in HDCA-6G levels. Such a change illustrates the efficacy of fenofibrate to stimulate bile acid glucuronidation (Fig. 6), an effect further confirmed by the strong induction of UGT2B4, UGT1A3 and UGT1A4 mRNA expression in PPARα-activated cells. Beyond UGTs, PPARα also up-regulates the multidrug resistance-associated protein (MRP)3 gene (41, 42). MRP3 is an efflux transporter involved in the basolateral secretion of glucuronide derivatives from hepatocytes (43, 44). Thus, not only does PPARα activation stimulate BA-G formation, but also their excretion into the systemic circulation where their concentration is significantly increased as evidenced in the present study (Fig. 6). Circulating BA-G are then removed by the kidneys and definitively eliminated in the urine (7, 45). Therefore, by activating the PPARα-dependent regulation of hepatic glucuronidation, fenofibrate stimulates a complete detoxification process allowing BA

excretion in the urine (Fig. 6). Such mechanism is of particular clinical relevance in the context of chronic cholestatic liver diseases, where BAs accumulate to toxic levels in hepatocytes due to an impaired biliary excretion (1) (Fig. 6). A series of small clinical trials recently revealed that fibrates, such as fenofibrate, improve liver biochemistries in PBC and PSC patients (8–13, 46). Our results suggest that this improvement reflects an increased BA glucuronidation and detoxification, in addition of the previously proposed anti-inflammatory and lipid-lowering mechanisms (14). This idea is supported by results from the pilot study involving 5 fenofibrate-treated PBC patients, in whom the drug also leads to an increase of serum BA-G levels. However, additional studies with larger PBC populations are required to validate the results from this pilot study, and more importantly, to establish the amplitude of BA-G modulation by fenofibrate in a cholestatic context.

In conclusion, these results provide the first clinical evidences that fenofibrate stimulate BA glucuronidation in humans. This effect reflects a PPARα-dependent activation of BA-conjugating UGTs in liver cells, and reduces bile acid toxicity in hepatocytes.

METHODS

Materials are detailed in the supplementary information (SI) 1.

Subjects

The non-cholestatic population for this study consisted of 300 Caucasian participants (150 men and 150 women) from the Genetics of Lipid Lowering Drugs and Diet Network (GOLDN). The study design, eligibility criteria, population demographics and laboratory characteristics have been extensively described previously (2) and are summarized in SI2. Briefly, participants were given 160 mg of fenofibrate/day (TriCor®, Abbott Laboratories, Chicago, IL) (2, 47). A 12H fast blood sample was drawn before and after the fenofibrate treatment period, and serum was isolated and frozen at −80°C until subsequent analyses (2).

The PBC samples were from patients attending the Liver Clinics at the University of Florida (Gainesville, FL) and at Mayo Clinic (Rochester, MN) (12). The population of the study consisted of 20 patients, but stored serum was available from only 5 of these patients (2 men and 3 women) for further BA-G measurement. The study design, eligibility criteria, population demographics and laboratory characteristics have been described previously (12) and are summarized in SI3. Briefly, patients with incomplete response to ursodeoxycholic acid (UDCA) were given 160 mg/day of the insoluble drug delivery-microparticle fenofibrate (IDD-P, Triglide, Sciele Pharma Inc. Atlanta, GA, USA) for 48 weeks, in addition to their usual dosages of daily UDCA (12). A 12H fast blood sample was drawn at entry and end of the study, and serum was isolated and frozen at −80°C until subsequent analyses (12).

The protocols were approved by the institutional review boards at the University of Minnesota (Minneapolis, MN), University of Florida (Gainesville, FL) and the CHU-Québec Research Centre (Québec, Canada). Written informed consent was obtained from all participants. All authors had access to the data of studies NCT00083369 and NCT00575042.

Analytical method

Concentrations of 11 BA-G (CDCA-3G and -24G, CA-24G, LCA-3G and -24G, DCA-3G and -24G, HDCA-6G and -24G and HCA-6G and -24G) were determined using high-performance liquid chromatography-tandem mass spectrometry (LC–MS/MS) as extensively described in SI1. The chromatographic system consisted of an Alliance 2690 HPLC instrument (Waters, Milford, MA), and the tandem mass spectrometry system (MS/MS) was an API4000 mass spectrometer (Applied Biosystems, Concord, Canada). As detailed in SI1, HCA-6G was quantified with a standard curve constructed using CDCA-3G. All other species were quantified with the appropriate standard curve. Limits of quantifications were: CDCA-3/24G, DCA-3/24G and HDCA-6/24G:1.76nM; LCA-3/24G: 1.81nM; and CA-24G and HCA-6/24G: 1.71nM.

GOLDN samples were also analyzed for a series of 17 unconjugated, taurine-, glycine- or sulfate-conjugated BA species using LC-MS/MS quantification (2) (see SI4). In the context of the present study, these concentrations were used to calculate the relative abundance (percentage) of BA-G and the metabolic ratio (MR) for each glucuronide.

UGT genotyping

Genomic DNA was isolated from peripheral blood leukocytes from the GOLDN study participants using Puregene DNA reagents according to the manufacturer's instructions (Qiagen, Germantown, MD, USA). Targeted UGT polymorphisms including UGT2B4 1374T>A (rs13119049, n=197), UGT2B7 802C>T (rs7439366, n=142), and UGT1A3 31T>C (rs3821242, n=227) were performed at the University of Minnesota BioMedical Genomics Center (http://www.bmgc.umn.edu/Genotyping/index.htm) using iPLEX Gold method and the previously reported genotyping strategies (21–23) (see SI1 for additional experimental informations).

Cell culture and mRNA level determination

Cryopreserved human primary hepatocytes from 3 donors (see SI1) were obtained from Celsis-InVitro Technologies (Baltimore, MD), and cultured as reported previously (17, 27). For RNA analyses, 350,000 hepatocytes/well were seeded in 12-well plates and cultured in the *Invitro Gro CP* medium for 48H. Cells were then treated with vehicle (DMSO, 0.1% v/v) or activators (250μM fenofibrate or 75μM Wy14,643) for 48H (17, 18). For glucuronide production 700,000 hepatocytes/well were seeded in 6-well plates, treated with vehicle (DMSO, 0.1% v/v) or Wy14,643 (75μM) for 48H, and then cultured with CDCA (100μM) for 2H. Culture media were analyzed for CDCA-3 and -24G through LC-MS/MS (see above). 10^6 HepG2 cells were treated as indicated with the PPARα activators, in the absence or presence of cycloheximide (20μg/mL) or actinomycin D (1μg/mL). Total RNA was isolated according to the Tri-Reagent acid: phenol protocol as specified by the supplier (Molecular Research Center Inc., Cincinnati, OH). The reverse transcription (RT) and quantitative PCR reactions were performed as previously described (17, 18, 27) and detailed in SI1.

MTS reduction assays and fluorescence-activated cell sorting

HepG2 cells (20,000cells/well) were seeded in 96-well plates, treated for 24–72H with 100μM BAs. MTS (3-(4,5-dimethylthiazol-2-yl)-5-(3-carboxymethoxyphenyl)-2-(4-sulfophenyl)-2H-tetrazolium) reduction was evaluated using the *CellTiter 96® AQueous One Solution Cell Proliferation Assay* according to the manufacturer's instructions (Promega, Madison, WI).

Living cell quantification was achieved through fluorescence-activated cell sorting (FACS) analyses using the annexin V/propidium iodide-co-labeling method as reported (48). Labeled cells were then analyzed using a BD FACSCanto II instrument (BD biosciences, San Jose, CA).

Production of HK293 cells overexpressing the UGT1A4 allozymes, microsomes isolation and western-blot analyses

HEK293 cells expressing the UGT1A4 T^{24}, V^{48} and W^{11} variant alleles were generated by site-directed mutagenesis of the wild type (WT) UGT1A4 ($R^{11}P^{24}L^{48}$)-pcDNA6v5-His vector (17, 26). UGT1A4-HK293 cell lines were obtained by transfecting 2 μg of the UGT1A4 plasmids with the ExGEN reagent according to manufacturer's instructions (Invitrogen). Stable transfectants were selected in medium containing 10 μg/mL blasticidin-HCl as previously described (17, 49). UGT2B7H^{268}- and Y^{268}-HEK293 cells were as described (25). Microsome pellets from UGT1A4- and UGT2B7-HEK293 cell lines were purified and resuspended at 5μg/μL as previously reported (17). For western-blot analyses, microsomal proteins (10μg) were size-separated by 10% SDS-PAGE, transferred onto nitrocellulose membranes, and then hybridized with anti-UGT1A (1:2,000) or anti-UGT2B (1:2,000) antibodies, as previously described (16, 17). An anti-rabbit IgG horse antibody (1:10,000) conjugated with peroxidase (Sigma, Mississauga, Canada) was used as the second antibody. Immunocomplexes were visualized on hyperfilm (Kodack Corp., Rochester, NY) and quantified by BioImage Visage 110s (Genomic Solution. Inc., Ann Harbor, MI). The same membranes were then rehybridized with an anti-calnexin (1:5,000) antibody (Stressgen) as a loading control assessment.

Glucuronidation assays

All assays were performed for 1H as previously reported (17, 36) using 100μM CDCA and 10μg of commercial bacculosomes, liver microsomes or microsomes purified from UGT1A4- and UGT2B7-HK293 cells. The formation of CDCA-3 and -24G was quantified by LC-MS/MS as described previously (36). Velocity values obtained with the UGT1A4 and UGT2B7 allozymes were normalized according to the UGT protein levels as determined by western-blot (WT proteins arbitrarily set at 1) (17, 26).

Data analyses

BA-G levels were calculated as mean±standard error of the mean (SEM) for non cholestatic volunteers or mean±standard deviation (SD) for PBC patients. BA-G concentrations did not satisfy the normal distribution according to the Shapiro-Wilk test, thus the matched pairs Wilcoxon signed-rank test was used for statistical analyses of the response to treatment. Comparisons of baseline profiles and the response to treatment between men and women,

were made using the Wilcoxon/Mann-Whitney rank-sum test (JMP V7.0.1,SAS Institute Inc, Cary, NC). For genotyping analyses, Hardy-Weinberg equilibrium was tested with the Allele Procedure in SAS, version 9.2 (SAS Institute Inc.). BA-G values were transformed before to normalize their distribution, and a repeated analysis of variance (ANOVA) model was used to evaluate the effect of each genotype and the genotype by response interaction effect (SAS Institute Inc.). These analyses were adjusted for the effects of age and sex.

The statistical significance of differences in mRNA levels, CDCA-24G formation and cell viability between control and treated cells, as well as in glucuronidation activity between WT and variants was determined through the nonparametric Student *t* test using the JMP V7.0.1 program (SAS Institute Inc.).

Supplementary Material

Refer to Web version on PubMed Central for supplementary material.

Acknowledgments

We wish to thank Dr. Virginie Bocher for critical reading of the manuscript. Bart Staels is a member of the “Institut Universitaire de France”. This study was supported by grants from the Canadian Institute of Health Research (CIHR; #MOP-84338 and -229488), the Canadian Liver Foundation and the Canadian Foundation for Innovation (CFI, #10469). The Genetics of Lipid Lowering Drugs and Diet Network (GOLDN) study was supported by the National Heart, Lung, and Blood Institute (National Institutes of Health) grant U 01 HL72524, Genetic and Environmental Determinants of Triglycerides. J. Trottier is holder of a scholarship from CIHR. M. Perreault is holder of a scholarship from the “Fonds pour la Recherche en Santé du Québec” (FRSQ). I. Rudkowska is supported by a CIHR-Bisby postdoctoral fellowship award (200810BFE). O. Barbier is holder of a salary grant from CIHR (New investigator #MSH95330) and FRSQ (junior II). M.-C. Vohl holds a Tier 1 Canada Research Chair in Genomics applied to Nutrition and Health.

References

1. Monte MJ, Marin JJ, Antelo A, Vazquez-Tato J. Bile acids: chemistry, physiology, and pathophysiology. World J Gastroenterol. 2009 Feb 21; 15(7):804–16. [PubMed: 19230041]
2. Trottier J, Caron P, Straka RJ, Barbier O. Profile of serum bile acids in noncholestatic volunteers: gender-related differences in response to fenofibrate. Clin Pharmacol Ther. 2011 Aug; 90(2):279–86. [PubMed: 21716269]
3. Pauli-Magnus C, Meier PJ. Hepatocellular transporters and cholestasis. J Clin Gastroenterol. 2005 Apr; 39(4 Suppl 2):S103–S10. [PubMed: 15758645]
4. Wagner M, Zollner G, Trauner M. Nuclear receptor regulation of the adaptive response of bile acid transporters in cholestasis. Semin Liver Dis. 2010 May; 30(2):160–77. [PubMed: 20422498]
5. Paumgartner G. Pharmacotherapy of cholestatic liver diseases. J Dig Dis. 2010; 11(3):119–25. [PubMed: 20579215]
6. Trottier J, Milkiewicz P, Kaeding J, Verreault M, Barbier O. Coordinate regulation of hepatic bile acid oxidation and conjugation by nuclear receptors. Mol Pharm. 2006 May-Jun;3(3):212–22. [PubMed: 16749854]
7. Barnabas A, Chapman RW. Primary sclerosing cholangitis: is any treatment worthwhile? Curr Gastroenterol Rep. 2012 Feb; 14(1):17–24. [PubMed: 22124849]
8. Dohmen K, Mizuta T, Nakamuta M, Shimohashi N, Ishibashi H, Yamamoto K. Fenofibrate for patients with asymptomatic primary biliary cirrhosis. World J Gastroenterol. 2004 Mar 15; 10(6): 894–8. [PubMed: 15040040]
9. Iwasaki S, Ohira H, Nishiguchi S, Zeniya M, Kaneko S, Onji M, et al. The efficacy of ursodeoxycholic acid and bezafibrate combination therapy for primary biliary cirrhosis: A prospective, multicenter study. Hepatol Res. 2008; 38(6):557–64. [PubMed: 18452482]

10. Nakai S, Masaki T, Kurokohchi K, Deguchi A, Nishioka M. Combination therapy of bezafibrate and ursodeoxycholic acid in primary biliary cirrhosis: a preliminary study. Am J Gastroenterol. 2000 Jan; 95(1):326–7. [PubMed: 10638623]

11. Ohira H, Sato Y, Ueno T, Sata M. Fenofibrate treatment in patients with primary biliary cirrhosis. Am J Gastroenterol. 2002; 97(8):2147–9. [PubMed: 12190200]

12. Levy C, Peter JA, Nelson DR, Keach J, Petz J, Cabrera R, et al. Pilot study: fenofibrate for patients with primary biliary cirrhosis and an incomplete response to ursodeoxycholic acid. Aliment Pharmacol Ther. 2011 Jan; 33(2):235–42. [PubMed: 21083674]

13. Chazouilleres, O., Corpechot, C., Gaouar, F., Poupon, R. AASLD. Fenofibrate improves liver tests in Primary Sclerosing Cholangitis with incomplete biochemical response to ursodeoxycholic acid. Hepatology; 61st Annual Meeting of the American-Association-for-the-Study-of-Liver-Diseases Oct 2010; Boston, MA. OCT 29-NOV 02, 2010; 2010. p. 488A

14. Staels B, Maes M, Zambon A. Fibrates and future PPARalpha agonists in the treatment of cardiovascular disease. Nature clinical practice Cardiovascular medicine. 2008 Sep; 5(9):542–53. Review.

15. Barbier O, Trottier J, Kaeding J, Caron P, Verreault M. Lipid-activated transcription factors control bile acid glucuronidation. Mol Cell Biochem. 2009 Jun; 326(1–2):3–8. [PubMed: 19130183]

16. Barbier O, Duran-Sandoval D, Pineda-Torra I, Kosykh V, Fruchart JC, Staels B. Peroxisome proliferator-activated receptor alpha induces hepatic expression of the human bile acid glucuronidating UDP-glucuronosyltransferase 2B4 enzyme. J Biol Chem. 2003 Aug 29; 278(35): 32852–60. [PubMed: 12810707]

17. Trottier J, Verreault M, Grepper S, Monté D, Bélanger J, Kaeding J, et al. Human UDP-glucuronosyltransferase (UGT)1A3 enzyme conjugates chenodeoxycholic acid in the liver. Hepatology. 2006; 44(5):1158–70. [PubMed: 17058234]

18. Senekeo-Effenberger K, Chen S, Brace-Sinnokrak E, Bonzo JA, Yueh MF, Argikar U, et al. Expression of the human UGT1 locus in transgenic mice by 4-chloro-6-(2,3-xylidino)-2-pyrimidinylthioacetic acid (WY-14643) and implications on drug metabolism through peroxisome proliferator-activated receptor alpha activation. Drug Metab Dispos. 2007

19. Holthe M, Rakvag TN, Klepstad P, Idle JR, Kaasa S, Krokan HE, et al. Sequence variations in the UDP-glucuronosyltransferase 2B7 (UGT2B7) gene: identification of 10 novel single nucleotide polymorphisms (SNPs) and analysis of their relevance to morphine glucuronidation in cancer patients. Pharmacogenomics J. 2003; 3(1):17–26. Comparative Study Research Support, Non-U.S. Gov't. [PubMed: 12629580]

20. Lampe JW, Bigler J, Bush AC, Potter JD. Prevalence of polymorphisms in the human UDP-glucuronosyltransferase 2B family: UGT2B4(D458E), UGT2B7(H268Y), and UGT2B15(D85Y). Cancer epidemiology, biomarkers & prevention : a publication of the American Association for Cancer Research, cosponsored by the American Society of Preventive Oncology. 2000 Mar; 9(3): 329–33. Research Support, Non-U.S. Gov't Research Support, U.S. Gov't, P.H.S.

21. Innocenti F, Liu W, Fackenthal D, Ramirez J, Chen P, Ye X, et al. Single nucleotide polymorphism discovery and functional assessment of variation in the UDP-glucuronosyltransferase 2B7 gene. Pharmacogenet Genomics. 2008 Aug; 18(8):683–97. Research Support, N.I.H., Extramural Research Support, Non-U.S. Gov't. [PubMed: 18622261]

22. Iwai M, Maruo Y, Ito M, Yamamoto K, Sato H, Takeuchi Y. Six novel UDP-glucuronosyltransferase (UGT1A3) polymorphisms with varying activity. J Hum Genet. 2004; 49(3):123–8. Research Support, Non-U.S. Gov't. [PubMed: 14986168]

23. Yong M, Schwartz SM, Atkinson C, Makar KW, Thomas SS, Newton KM, et al. Associations between polymorphisms in glucuronidation and sulfation enzymes and mammographic breast density in premenopausal women in the United States. Cancer epidemiology, biomarkers & prevention : a publication of the American Association for Cancer Research, cosponsored by the American Society of Preventive Oncology. 2010 Feb; 19(2):537–46. Research Support, N.I.H., Extramural Research Support, Non-U.S. Gov't.

24. Caillier B, Lépine J, Tojcic J, Ménard V, Pérusse L, Bélanger A, et al. A pharmacogenomics study of the human estrogen glucuronosyltransferase UGT1A3. Pharmacogenet Genomics. 2007 Jul; 17(7):481–95. [PubMed: 17558304]

25. Coffman BL, King CD, Rios GR, Tephly TR. The glucuronidation of opioids, other xenobiotics, and androgens by human UGT2B7Y(268) and UGT2B7H(268). Drug Metab Dispos. 1998 Jan; 26(1):73–7. [PubMed: 9443856]
26. Laverdière I, Caron P, Harvey M, Lévesque E, Guillemette C. In vitro investigation of human UDP-glucuronosyltransferase isoforms responsible for tacrolimus glucuronidation: predominant contribution of UGT1A4. Drug Metab Dispos. 2011 Jul; 39(7):1127–30. [PubMed: 21487055]
27. Verreault M, Senekeo-Effenberger K, Trottier J, Bonzo JA, Bélanger J, Kaeding J, et al. The liver X-receptor alpha controls hepatic expression of the human bile acid-glucuronidating UGT1A3 enzyme in human cells and transgenic mice. Hepatology. 2006; 44(2):368–78. [PubMed: 16871576]
28. Takikawa H, Minagawa K, Sano N, Yamanaka M. Lithocholate-3-O-glucuronide-induced cholestasis. A study with congenital hyperbilirubinemic rats and effects of ursodeoxycholate conjugates. Dig Dis Sci. 1993 Aug; 38(8):1543–8. Comparative Study. [PubMed: 8344113]
29. Gall WE, Zawada G, Mojarrabi B, Tephly TR, Green MD, Coffman BL, et al. Differential glucuronidation of bile acids, androgens and estrogens by human UGT1A3 and 2B7. J Steroid Biochem Mol Biol. 1999 Jul-Aug;70(1–3):101–8. [PubMed: 10529008]
30. Caron P, Trottier J, Verreault M, Bélanger J, Kaeding J, Barbier O. Enzymatic production of bile Acid glucuronides used as analytical standards for liquid chromatography-mass spectrometry analyses. Mol Pharm. 2006 May-Jun;3(3):293–302. [PubMed: 16749861]
31. Hofmann AF. Why bile acid glucuronidation is a minor pathway for conjugation of endogenous bile acids in man. Hepatology. 2007; 45(4):1083–4. [PubMed: 17393523]
32. Regan SL, Maggs JL, Hammond TG, Lambert C, Williams DP, Park BK. Acyl glucuronides: the good, the bad and the ugly. Biopharm Drug Dispos. 2010 Oct; 31(7):367–95. [PubMed: 20830700]
33. Shipkova M, Armstrong VW, Oellerich M, Wieland E. Acyl glucuronide drug metabolites: toxicological and analytical implications. Ther Drug Monit. 2003 Feb; 25(1):1–16. [PubMed: 12548138]
34. Zhang D, Raghavan N, Wang L, Xue Y, Obermeier M, Chen S, et al. Plasma stability-dependent circulation of acyl glucuronide metabolites in humans: how circulating metabolite profiles of muraglitazar and peliglitazar can lead to misleading risk assessment. Drug Metab Dispos. 2011 Jan; 39(1):123–31. [PubMed: 20876787]
35. Buckley DB, Klaassen CD. Mechanism of gender-divergent UDP-glucuronosyltransferase mRNA expression in mouse liver and kidney. Drug Metab Dispos. 2009 Apr; 37(4):834–40. [PubMed: 19131521]
36. Trottier J, El Husseini D, Perreault M, Pâquet S, Caron P, Bourassa S, et al. The human UGT1A3 enzyme conjugates norursodeoxycholic acid into a C23-ester glucuronide in the liver. J Biol Chem. 2010 Jan 8; 285(2):1113–21. [PubMed: 19889628]
37. Verreault M, Kaeding J, Caron P, Trottier J, Grosse L, Houssin E, et al. Regulation of endobiotics glucuronidation by ligand-activated transcription factors: physiological function and therapeutic potential. Drug Metab Rev. 2010 Feb; 42(1):110–22. [PubMed: 19831728]
38. Erichsen TJ, Aehlen A, Ehmer U, Kalthoff S, Manns MP, Strassburg CP. Regulation of the human bile acid UDP-glucuronosyltransferase 1A3 by the farnesoid X receptor and bile acids. J Hepatol. 2010 Apr; 52(4):570–8. Research Support, Non-U.S. Gov't. [PubMed: 20189675]
39. Lévesque E, Beaulieu M, Hum DW, Bélanger A. Characterization and substrate specificity of UGT2B4 (E458): a UDP-glucuronosyltransferase encoded by a polymorphic gene. Pharmacogenetics. 1999; 9(2):207–16. [PubMed: 10376768]
40. Lévesque E, Ménard V, Laverdière I, Bellemare J, Barbier O, Girard H, et al. Extensive splicing of transcripts encoding the bile acid-conjugating enzyme UGT2B4 modulates glucuronidation. Pharmacogenet Genomics. 2010 Mar; 20(3):195–210. [PubMed: 20139797]
41. Moffit JS, Aleksunes LM, Maher JM, Scheffer GL, Klaassen CD, Manautou JE. Induction of hepatic transporters multidrug resistance-associated proteins (Mrp) 3 and 4 by clofibrate is regulated by peroxisome proliferator-activated receptor alpha. J Pharmacol Exp Ther. 2006 May; 317(2):537–45. [PubMed: 16467456]

42. Maher JM, Cheng X, Slitt AL, Dieter MZ, Klaassen CD. Induction of the multidrug resistance-associated protein family of transporters by chemical activators of receptor-mediated pathways in mouse liver. Drug Metab Dispos. 2005 Jul; 33(7):956–62. [PubMed: 15833929]
43. Hirouchi M, Kusuhara H, Onuki R, Ogilvie BW, Parkinson A, Sugiyama Y. Construction of triple-transfected cells [organic anion-transporting polypeptide (OATP) 1B1/multidrug resistance-associated protein (MRP) 2/MRP3 and OATP1B1/MRP2/MRP4] for analysis of the sinusoidal function of MRP3 and MRP4. Drug Metab Dispos. 2009 Oct; 37(10):2103–11. [PubMed: 19628752]
44. Zein CO, Lindor KD. Latest and emerging therapies for primary biliary cirrhosis and primary sclerosing cholangitis. Curr Gastroenterol Rep. 2010 Feb; 12(1):13–22. [PubMed: 20425480]
45. Pauli-Magnus C, Stieger B, Meier Y, Kullak-Ublick GA, Meier PJ. Enterohepatic transport of bile salts and genetics of cholestasis. J Hepatol. 2005 Aug; 43(2):342–57. [PubMed: 15975683]
46. Iwasaki S, Akisawa N, Saibara T, Onishi S. Fibrate for treatment of primary biliary cirrhosis. Hepatol Res. 2007 Oct; 37(Suppl 3):S515–S7. [PubMed: 17931214]
47. Lai CQ, Arnett DK, Corella D, Straka RJ, Tsai MY, Peacock JM, et al. Fenofibrate effect on triglyceride and postprandial response of apolipoprotein A5 variants: the GOLDN study. Arterioscler Thromb Vasc Biol. 2007 Jun; 27(6):1417–25. [PubMed: 17431185]
48. Rieger AM, Nelson KL, Konowalchuk JD, Barreda DR. Modified annexin V/propidium iodide apoptosis assay for accurate assessment of cell death. Journal of visualized experiments : JoVE. [Research Support, Non-U.S. Gov't Video-Audio Media]. 2011; (50)
49. Benoit-Biancamano MO, Adam JP, Bernard O, Court MH, Leblanc MH, Caron P, et al. A pharmacogenetics study of the human glucuronosyltransferase UGT1A4. Pharmacogenet Genomics. 2009 Nov 3.19:945–54. [PubMed: 19890225]
50. Shen J, Arnett DK, Parnell LD, Peacock JM, Lai CQ, Hixson JE, et al. Association of common C-reactive protein (CRP) gene polymorphisms with baseline plasma CRP levels and fenofibrate response: the GOLDN study. Diabetes Care. 2008 May; 31(5):910–5. [PubMed: 18285551]

STUDY HIGHLIGHTS

What is current knowledge on the topic?

- Toxic bile acids (BA) accumulate in the cholestatic liver.
- Glucuronidation, catalyzed by UDP-glucuronosyltransferase (UGT) enzymes, detoxifies BAs
- Fenofibrate ameliorates liver biochemistries in cholestatic patients.

What question this study addressed?

- Does fenofibrate stimulates BA glucuronidation in humans?

What this study adds to our knowledge?

This study provides:

- Clinical evidences that circulating BA-Gs are affected by gender and genetic mutations in UGT genes,
- A clear picture of the contribution of human UGT enzymes in BA glucuronidation.
- A first clinical assessment of the fenofibrate-dependent stimulation of BA glucuronidation in clinics.
- A pharmacological explanation of these effects.

How this might change clinical pharmacology and therapeutics

- The present study further supports the use of fibrate drugs for chronic cholestasis, and supports the search for more potent inducers of BA glucuronidation for cholestasis treatment.

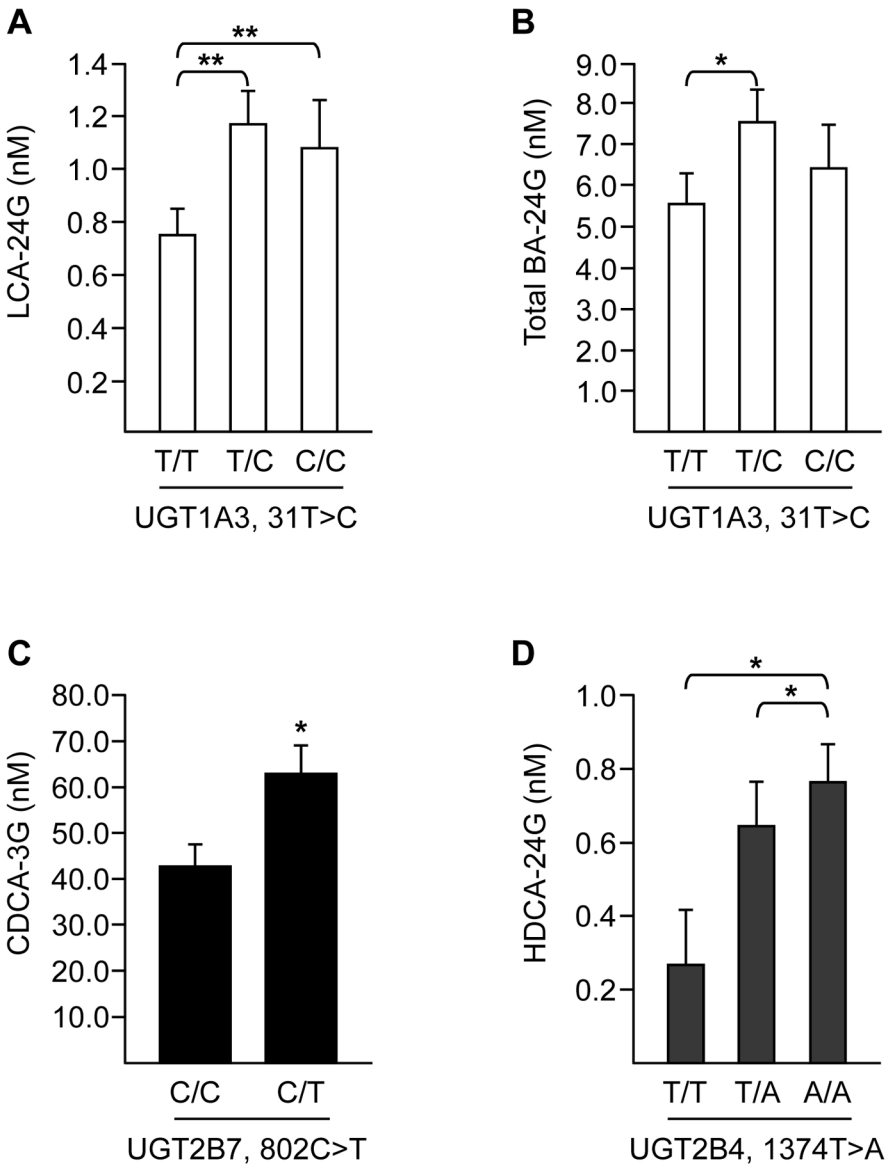

Figure 1. Effects of the UGT1A3 31T>C (A&B), UGT2B7 802C>T (C) and UGT2B4 1374T>A (D) polymorphisms on baseline serum levels of LCA-24G (A), total bile acid-24glucuronides (B), CDCA-3G (C) and HDCA-24G (D)

Bile acid glucuronide levels were determined through LC-MS/MS analyses as described in the experimental procedure and SI1 sections. Genomic DNA was isolated from peripheral blood leukocytes and genotyped for the UGT1A3 31T>C (n=227 donors, **A&B**), UGT2B7 802C>T (n=142 donors, **C**) and UGT2B4 1374T>A (n=197 donors, **D**) mutations. All values represent the mean±SEM. A repeated analysis of variance (ANOVA) model was used to evaluate the effect of each genotype: *, $p<0.05$; **, $p<0.01$. All analyses were adjusted for the effects of age and sex. Only significant associations are shown, while the complete results are provided in supplementary informations 5–7.

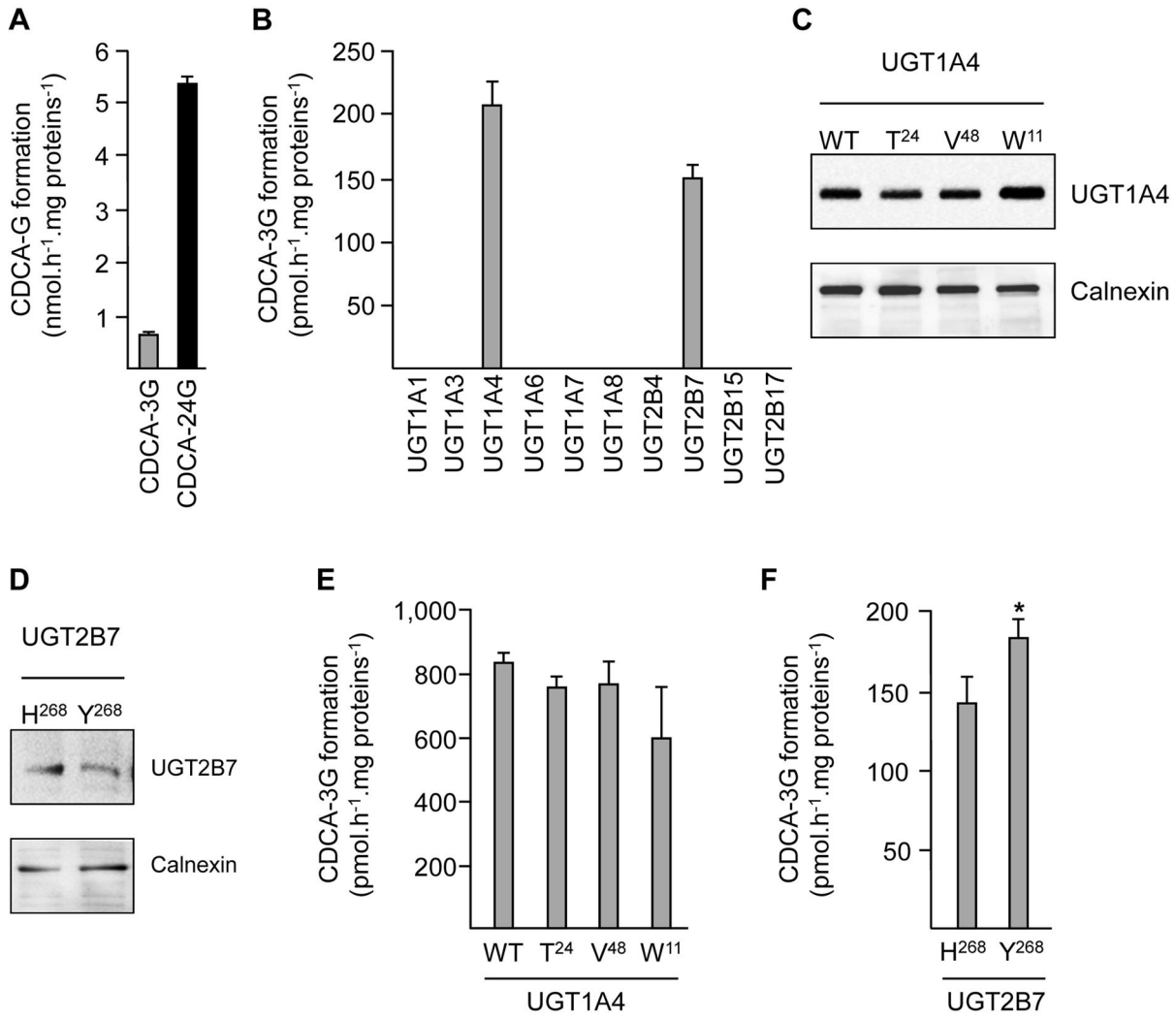

Figure 2. UGT1A4 and UGT2B7 catalyze the conversion of CDCA into CDCA-3G

(**A**) Ten μg of human liver microsomes were incubated in the presence of CDCA and the quantification of the two CDCA-glucuronides was achieved by LC-MS/MS.

(**B**) The formation of CDCA-3G by UGT-bacculosomes (10μg) was analyzed by LC-MS/MS.

(**C & D**) The UGT protein contents in microsomes from UGT1A4− **(C)** or UGT2B7-HEK293 (**D**) cell clones were compared by western blot experiments using the anti-UGT1A (**D**, 1:2,000) or the anti-UGT2B (**D**, 1:2000) antibodies. The equal loading of each lane was ensured by hybridizing with an anti-calnexin antibody (1:5,000; bottom panels).

(**E & F**) The formation of CDCA-3G by microsomes (10μg) from HK293 cells over-expressing each of the 4 UGT1A4 (**E,** WT, T^{24}, V^{48} and W^{11}) or the 2 UGT2B7 (**F,** WT and Y^{268}) allele variants was quantified by LC-MS/MS, and normalized according to the UGT protein level in the microsomal extract as determined by western-blot (**C & D**, WT proteins were arbitrarily set at 1)

All assays were performed for 1H at 37°C in the presence of 100μM CDCA and 2mM of the co-substrate UDP-Glucuronic Acid (UDPGA). Data represent the mean ± S.D. The

statistical significance of differences in glucuronidation activity between wild type and UGT variants was determined through the nonparametric Student *t* test (*, $p<0.05$).

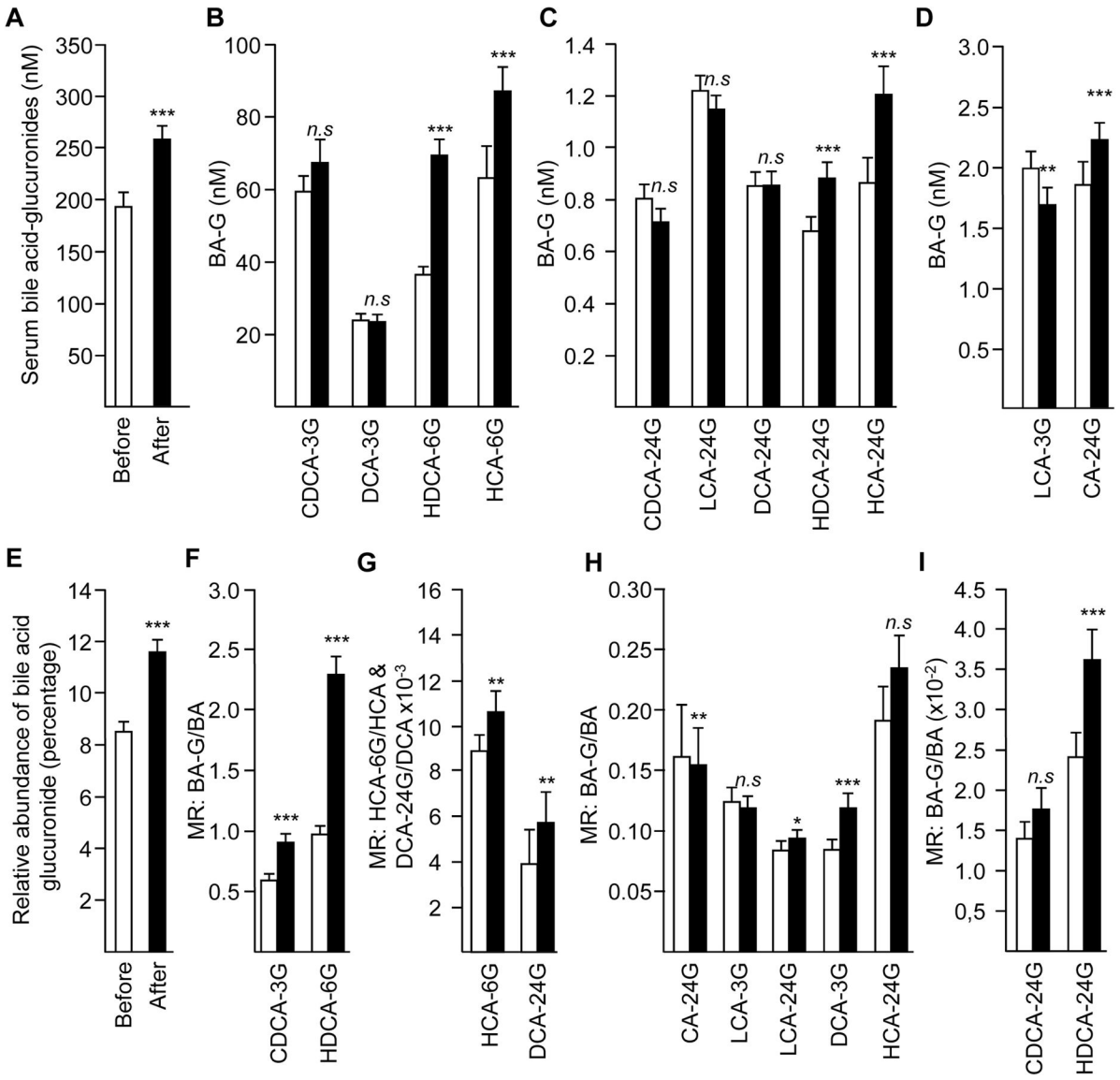

Figure 3. Differential modulation of serum bile acid glucuronides (A–D), their relative abundance (E) and metabolic ratios (F–I) in 300 non-cholestatic volunteers after 3-week treatment with fenofibrate

Three hundred volunteers (150 women and 150 men) were given a 3-week treatment with fenofibrate. Serum bile acids were determined through LC-MS/MS measurements in serum drawn before (white bars) and after (black bars) fenofibrate exposure. All values represent the mean±SEM. (**A**) The serum bile acid-glucuronides level is calculated as the sum of all bile acid glucuronide species.

(**E**) The relative abundance of glucuronide conjugates (**A**) was calculated as the ratio of total BA-G versus total BA + total BA-G, and is expressed as percentage. Concentrations of unconjugated acids (SI4) were determined as reported (2).

(**F**–**I**) The metabolic ratio for each species (**B**–**F**) was calculated as the ratio of glucuronide *versus* unconjugated precursor.

Statistically significant differences in pre- *versus* post-fenofibrate samples were determined using the Wilcoxon matched-pairs signed-ranks test: *, $p<0.05$; **, $p<0.01$; ***, $p<0.001$; *n.s*: not significant.

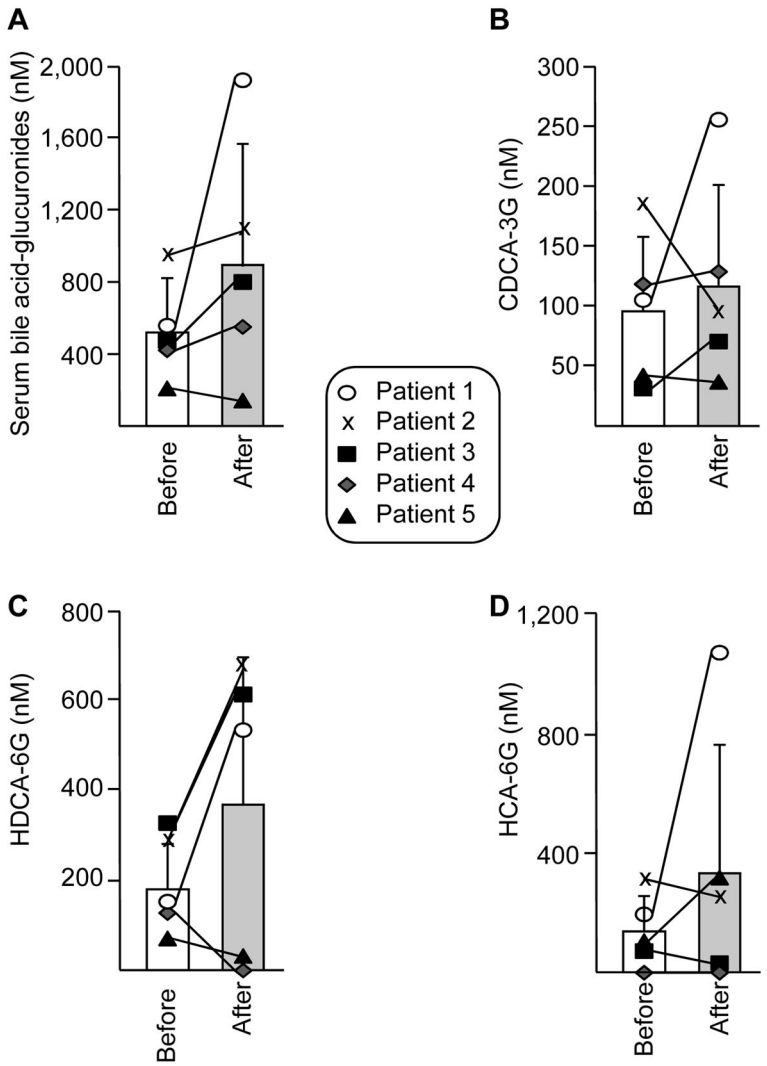

Figure 4. A 48-week treatment period with fenofibrate tend to increase the total bile acid glucuronides (A), CDCA-3G (B), HDCA-6G (C) and HCA-6G (D) levels in sera from 5 patients with Primary Biliary Cirrhosis

Serum bile acid glucuronides were determined in serum samples from each donor, drawn before (white bars) and after (gray bars) a 48-week fenofibrate exposure. Individual levels are illustrated, and bars represent the mean±SD. Statistically significant differences between pre- and post-treatment bile acid-glucuronide concentrations were analyzed using the Wilcoxon/Mann-Whitney rank sum test: no statistical differences were detected.

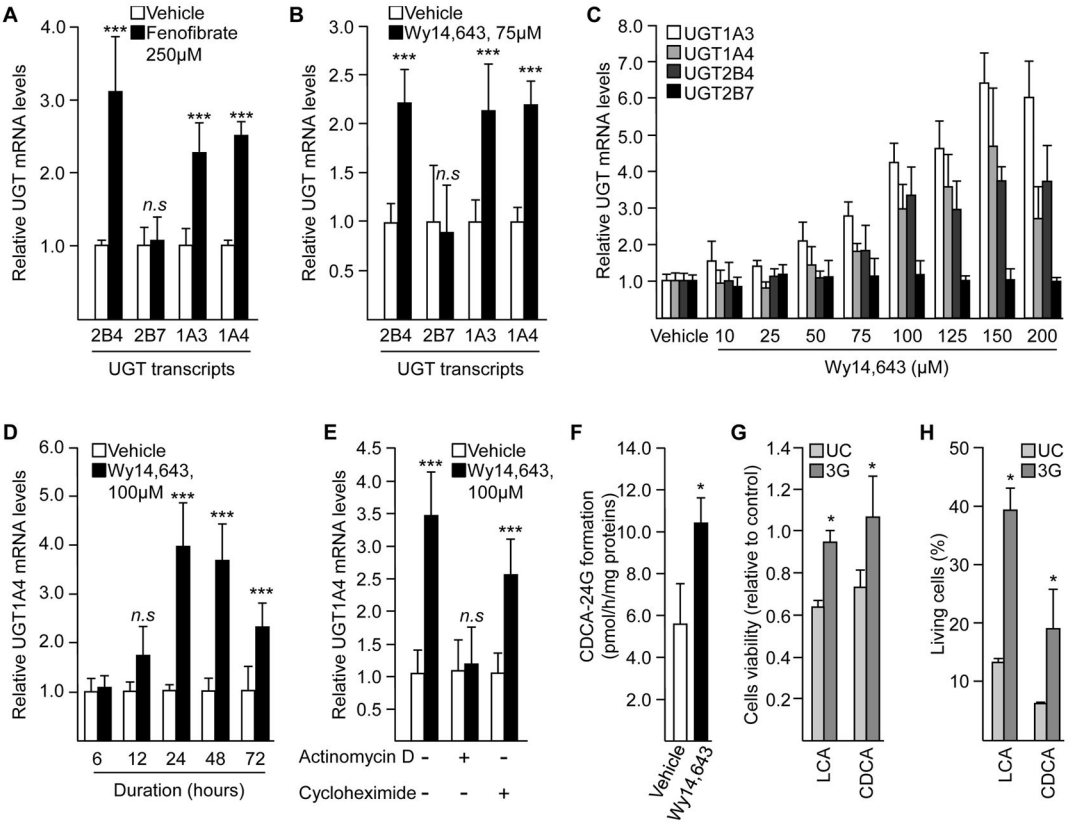

Figure 5. The PPARα agonists Fenofibrate (A) and Wy14,643 (B–E) differentially affects expression of the human bile acid-conjugating UGTs in human hepatocytes (A & B) and hepatoma HepG2 cells (C–E), and increases CDCA glucuronidation (F, hepatocytes), while 3glucuronide conjugates of LCA and CDCA are less cytotoxic than their unconjugated precursors for HepG2 cells (G & H)

(**A, B & F**) Primary human hepatocytes (SI1) were treated for 48H with DMSO (vehicle), fenofibric acid 250μM (donor 1, **A**) or Wy14,643 75μM (donors 2, **B & 3, F**).

(**C**) HepG2 cells were treated for 48H with DMSO (Vehicle) or increasing doses (10–200 μM) of Wy14,643.

(**D**) HepG2 cells were treated with DMSO (Vehicle) or Wy14,643 (100 μM) for increasing durations (6–72H).

(**E**) HepG2 cells were incubated for 48H with DMSO (Vehicle) or Wy14,643 (100μM) in the absence or presence of cycloheximide (20μg/mL) or actinomycin D (1μg/mL).

(**A–E**) UGT2B4 (**A–C**), UGT2B7 (**A–C**), UGT1A3 (**A–C**) and UGT1A4 (**A–E**) mRNA levels were measured by real-time PCR and expressed relative over control (vehicle) set at 1 (SI1). All values represent the mean±SD.

(**F**) CDCA-24G was quantified in culture media from vehicle- and Wy14,643-treated hepatocytes by LC-MS/MS and normalized according to the protein content in corresponding cell homogenates.

(**G & H**) HepG2 cells were exposed to vehicle (DMSO), 100μM unconjugated (UC) or glucuronidated (3G) forms of lithocholic (LCA) and chenodeoxycholic (CDCA) for 48 (**G**), 24 (**H**, LCA and LCA-3G) or 72H (**H**, CDCA and CDCA-3G). Living cells were determined using the MTS reduction assay (**H**) and living cells were quantified through fluorescence-

activated cell sorting analyses (**G**). The relative abundance (expressed as percentage) of living cell populations were determined by dividing their quartiles by the total cell population (**G**). All values represent the mean±SD.

Statistically significant differences in vehicle versus treated samples, and in glucuronide- versus unconjugated-exposed cells were determined using the Student *t* test: *, $p<0.05$; ***, $p<0.001$; n.s: not significant). While not shown for an easier viewing, the increase in UGT mRNA levels observed in the dose response experiment (**C**) became and remained statistically significant ($p<0.05$) at Wy14,643 concentrations above 10μM (UGT1A3) or 75μM (UGT1A4 and UGT2B4).

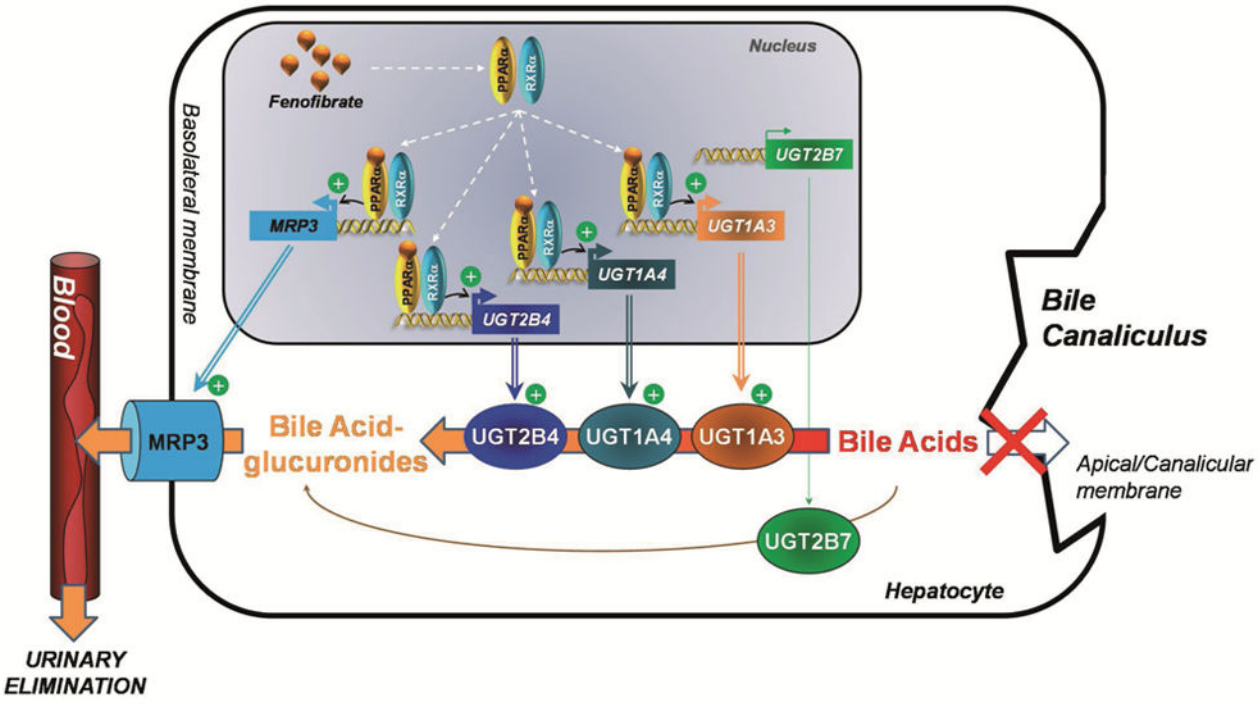

Figure 6. Proposed mechanism of action for the fenofibrate-dependent stimulation of bile acids detoxification in the cholestatic liver

In cholestatic liver cells, fenofibrate activates the nuclear receptor PPARα, which then form an active heterodimer with its partner RXR, and activates the regulatory regions of several target genes, including the BA-conjugating enzymes UGT2B4, UGT1A3 and UGT1A4 and the glucuronide efflux transporter, MRP3 (16–18, 41, 42) (Fig. 5). By contrast, the fenofibrate-activated receptor does not bind to nor activate the UGT2B7 gene. The increased UGT1A3 (17) (Fig. 5), UGT1A4 (Fig. 5) and UGT2B4 (16) (Fig. 5) enzymes conjugate the accumulating bile acids that cannot be excreted in the bile canaliculus due to bile flow impairment. The resulting bile acid-glucuronides are then secreted into the blood through the increased MRP3 protein (41–43) at the basolateral membrane of the cells. Glucuronides accumulate in the blood (Fig. 3 and Table 1), before being removed by the kidneys and definitively eliminated in the urine (7, 45). Thus, fenofibrate stimulates a complete detoxification process which reduces the burden of toxic acids in the liver, an effect that may participate to the reported improvement of liver functioning in treated-cholestatic patients (8, 11–13).

BA: Bile acids; PPARα: Peroxisome Proliferator-Activated Receptor alpha; RXR: Retinoid X-Receptor (RXR); UGT: UDP-glucuronosyltransferase; MRP: multidrug resistance-associated protein.

Table 1

Gender differences in the baseline profile of serum bile acid glucuronides in the GOLDN population

Serum levels	♂ + ♀ (n=300)	♂ (n=150)	♀ (n=150)
CDCA-3G	59.6 ± 4.2	72.7 ± 7.3	46.4 ± 3.9***
CDCA-24G	0.8 ± 0.1	0.9 ± 0.1	0.7 ± 0.1
CA-24G	1.9 ± 0.2	2.1 ± 0.3	1.6 ± 0.1
LCA-3G	2.0 ± 0.1	2.3 ± 0.2	1.6 ± 0.1*
LCA-24G	1.2 ± 0.1	1.3 ± 0.1	1.1 ± 0.1
DCA-3G	24.3 ± 1.6	27.9 ± 2.6	20.6 ± 1.7
DCA-24G	0.9 ± 0.1	0.9 ± 0.1	0.8 ± 0.1
HDCA-6G	36.7 ± 2.1	42.6 ± 3.5	30.7 ± 2.1*
HDCA-24G	0.7 ± 0.1	0.7 ± 0.1	0.7 ± 0.1
HCA-6G	63.5 ± 8.6	81.9 ± 16.2	45.1 ± 5.3***
HCA-24G	0.9 ± 0.1	1.0 ± 0.1	0.8 ± 0.1
TOTAL	192.3 ± 13.1	234.4 ± 24.9	150.1 ± 8.8***
Metabolic ratios			
CDCA-3G/CDCA	0.60 ± 0.05	0.58 ± 0.07	0.63 ± 0.07
CDCA-24G/CDCA	0.01 ± 0.00	0.01 ± 0.00	0.02 ± 0.01
CA-24G/CA	0.16 ± 0.04	0.23 ± 0.08	0.09 ± 0.02
LCA-3G/LCA	0.12 ± 0.01	0.14 ± 0.02	0.11 ± 0.01
LCA-24G/LCA	0.08 ± 0.01	0.08 ± 0.01	0.09 ± 0.01
DCA-3G/DCA	0.08 ± 0.01	0.10 ± 0.01	0.07 ± 0.01
DCA-24G/DCA	0.01 ± 0.00	0.01 ± 0.00	0.01 ± 0.00
HDCA-6G/HDCA	0.98 ± 0.06	1.06 ± 0.09	0.91 ± 0.09*
Metabolic ratios			
HDCA-24G/HDCA	0.02 ± 0.01	0.03 ± 0.01	0.02 ± 0.01
HCA-6G/HCA	8.90 ± 0.69	9.02 ± 0.93	8.89 ± 0.89
HCA-24G/HCA	0.19 ± 0.03	0.18 ± 0.04	0.19 ± 0.03

Bile acid-glucuronide concentrations are expressed in nM. Values represent the mean±SEM. The metabolic ratio for each species was calculated as the ratio of glucuronide *versus* unconjugated precursor (SI4). Statistically significant differences between male and female serum samples were determined by the rank-sum Wilcoxon/Mann-Whitney test:

*: $p<0.05$;

***: $p<0.001$.

CA: cholic acid; CDCA: chenodeoxycholic acid; DCA: deoxycholic acid; HCA: hyocholic acid; HDCA: hyodeoxycholic acid; LCA: lithocholic acid; G: glucuronide. TOTAL: sum of all bile acid glucuronides.